Proton spin–lattice relaxation in vinyl polymers

F. Heatley and M. K. Cox
Chemistry Department, University of Manchester, Manchester M13 9PL, UK
(Received 9 September 1976; revised 2 November 1976)

Proton spin–lattice relaxation times and Overhauser enhancements in vinyl polymers have been calculated for three correlation time distributions, and compared with experimental measurements on solutions of poly(vinyl acetate) in toluene-d_8. The results show that of the models considered, only the conformational jump model offers a consistently successful interpretation of the polymer motion.

INTRODUCTION

Nuclear spin–lattice relaxation in polymers arises almost entirely from intramolecular dipole–dipole interactions modulated by the polymer motion. For flexible random coil chains in solution, such as vinyl polymers or polyethers, reorientation of internuclear vectors proceeds by a number of processes, ranging from rapid small scale conformational jumps to slow overall tumbling of the whole polymer molecule. This variety of motions is manifest in n.m.r. relaxation experiments in the observation[1–5] that the relaxation data cannot be explained by the single correlation time model of molecular motion, but instead require the assumption of either a distribution of correlation times[1,3,5] or a combination of two motions with different correlation times[2,3,6]. ^{13}C relaxation studies[1,3,4] have been most important in characterizing the correlation time distribution, but it has been shown[3] that for a given system it is generally possible to explain the results by several different models. We have therefore investigated the possibility of measuring proton relaxation times, in addition to ^{13}C data, in order to characterize polymer motion more precisely. Since almost all polymers contain protons, such a technique would be applicable to polymers of widely different structures and flexibilities. Moreover, previous studies[7,8] have shown that intermolecular contributions to polymer relaxation are negligible.

The significance of proton relaxation is however greater than its practical convenience. To determine polymer motion fully, one would like to measure autocorrelation functions $G(\tau)$, for reorientation of an internuclear vector. N.m.r. relaxation measurements cannot provide $G(\tau)$ but only a few points in the frequency domain via the spectral density function $J(\omega)$ defined by:

$$J(\omega) = \frac{1}{2} \int_{-\infty}^{\infty} G(\tau) e^{(i\omega\tau)} d\tau$$

where $G(\tau)$ is the normalized second order spherical harmonic autocorrelation function. The ^{13}C spin–lattice relaxation time T_{1C} of a $^{13}CH_n$ group provides information on $J(\omega_H - \omega_C)$, $J(\omega_C)$ and $J(\omega_H + \omega_C)$ through the relationship[9]:

$$\frac{1}{T_{1C}} = \left[\frac{\mu_0}{4\pi}\right]^2 \left[\frac{n\gamma_C^2\gamma_H^2\hbar^2}{10R_{CH}^6}\right] [J(\omega_H - \omega_C) + 3J(\omega_C) + 6J(\omega_H + \omega_C)] \qquad (1)$$

where ω_H and ω_C are the ^1H and ^{13}C resonance frequencies and R_{CH} is the C–H bond length. Since ω_H and ω_C differ by a factor of 4, typically 100 and 25 MHz, measurements of T_{1C} sample $J(\omega)$ at frequencies in the MHz region. However, for two different protons, H_A and H_X, the relation time T_{1H} due to their mutual interaction is given approximately (see next section) by:

$$\frac{1}{T_{1H}} = \left[\frac{\mu_0}{4\pi}\right]^2 \left[\frac{\gamma_H^4\hbar^2}{10R_{AX}^6}\right] [J(\omega_A - \omega_X) + 3J(\omega_A) + 6J(\omega_A + \omega_X)] \qquad (2)$$

Now ω_A and ω_X differ by only a few hundred Hz at the most, so that T_{1H} samples $J(\omega)$ at very low frequencies as well as at high frequencies. Proton spin–lattice relaxation times therefore are a means of probing the polymer motion at frequencies far removed from the normal resonance frequencies. An alternative way of sampling $J(\omega)$ at low frequencies is to measure spin–spin lattice relaxation times (T_2) which depend[9] on $J(0)$. However, such uncertainties as tacticity, field inhomogeneity and residual spin–spin coupling prevent accurate measurement of T_2 from linewidths of polymers in solution, and there are a number of sources of systematic error[10] in the measurement of T_2 in spin-coupled systems by the spin-echo technique.

THEORY AND RESULTS OF CALCULATIONS

Basic theory

We consider here only vinyl polymers $(-CH_2-CHZ-)_m$ in which there are no magnetic interactions between the backbone protons and the side group Z. If S_A and S_X represent the total methine and methylene longitudinal magnetizations respectively, then the spin–lattice relaxation is governed by the phenomenological equations[11]:

$$\frac{\mathrm{d}S_A}{\mathrm{d}t} = -\frac{(S_A - S_A^0)}{T_{AA}} - \frac{(S_X - S_X^0)}{T_{AX}} \tag{3a}$$

$$\frac{\mathrm{d}S_X}{\mathrm{d}t} = -\frac{(S_X - S_X^0)}{T_{XX}} - \frac{(S_A - S_A^0)}{T_{XA}} \tag{3b}$$

where the superscript zero denotes values at thermal equilibrium. The time constants T_{AA}, T_{XX}, T_{AX} and T_{XA} depend on the interproton distances as well as on the rate of molecular motion. Molecular models showed that in certain accessible conformations, there are significant interactions between protons separated by 4 and 5 bonds, as well as between *geminal* and vicinal protons. Assuming only intramolecular contributions to the relaxation, the time constants are therefore given by:

$$\frac{1}{T_{AA}} = K\left(\frac{6J(\omega_A) + 24J(2\omega_A)}{R_{AA}^6}\right) + \left(\frac{4J(\omega_A - \omega_X) + 12J(\omega_A) + 24J(\omega_A + \omega_X)}{R_{AX}^6}\right)$$

$$\frac{1}{T_{XX}} = K\left(\frac{3J(\omega_X) + 12J(2\omega_X)}{R_{XX}^6}\right) + \left(\frac{2J(\omega_A - \omega_X) + 6J(\omega_X) + 12J(\omega_A + \omega_X)}{R_{AX}^6}\right)$$

$$\frac{1}{T_{AX}} = \frac{1}{2T_{XA}} = K\left(\frac{6J(\omega_A + \omega_X) - J(\omega_A - \omega_X)}{R_{AX}^6}\right)$$

where $K = (\mu_0/4\pi)^2(\gamma_H^4\hbar^2/10)$.

R_{AA} is an effective A–A distance defined by:

$$\frac{1}{R_{AA}^6} = \left(\frac{1}{R_{AA}^{(1)}}\right)^6 + \left(\frac{1}{R_{AA}^{(2)}}\right)^6 + \ldots$$

where $R_{AA}^{(1)}$ is the average distance between nearest neighbour methine protons, $R_{AA}^{(2)}$ the average distance between next nearest methines, and so on. R_{AX} is defined in the same way as R_{AA}, but R_{XX} is slightly different:

$$\frac{1}{R_{XX}^6} = \left(\frac{1}{R_{XX}^g}\right)^6 + 4\left[\left(\frac{1}{R_{XX}^{(1)}}\right)^6 + \left(\frac{1}{R_{XX}^{(2)}}\right)^6 + \cdots\right]$$

R_{XX}^g is the *geminal* methylene proton separation, $R_{XX}^{(1)}$ is the average distance between methylene protons in nearest neighbour groups, and so on. The determination of these distances is described in a later section. The assumption of identical autocorrelation functions for all dipolar interactions is justified firstly by the experimental results described below, and secondly by the short range (2–3 monomer units) character of all the dominant interactions.

The functions $J(\omega)$ depend on the reorientational model employed and are discussed in more detail below. First we must apply the master equations (4a) and (4b) to the conditions applicable to a particular experiment. Three such experiments are described here which can be performed easily on most Fourier transform spectrometers without modification. The experiments are: (a) the standard inversion recovery (i.r.) technique using the π–τ–$\pi/2$ sequence, where the π pulse inverts all signals in the spectrum (non-selective) and there are no perturbing fields (b) the i.r. experiment in which one nucleus is saturated by a decoupling field, and (c) ^{1}H–{^{1}H} nuclear Overhauser effect (*NOE*) measurements.

Unperturbed i.r. experiment. The recovery of S_A and S_X is governed by the coupled differential equations (3a) and (3b). Solution of these yields:

$$S_A - S_A^0 = P\exp(-t/T_+) + Q\exp(-t/T_-) \tag{4a}$$

$$S_X - S_X^0 = P'\exp(-t/T_+) + Q'\exp(-t/T_-) \tag{4b}$$

where:

$$\frac{1}{T_\pm} = \frac{1}{2}\left\{\left(\frac{1}{T_{AA}} + \frac{1}{T_{XX}}\right) \pm \left[\left(\frac{1}{T_{AA}} + \frac{1}{T_{XX}}\right)^2 - 4\left(\frac{1}{T_{AA}T_{XX}} - \frac{1}{T_{AX}T_{XA}}\right)\right]^{1/2}\right\}$$

$$P = \frac{2S_A^0(T_{AX}/T_- - T_{AX}/T_{AA}) - 2S_X^0}{(T_{AX}/T_+ - T_{AX}/T_-)}$$

$$Q = \frac{2S_A^0(T_{AX}/T_+ - T_{AX}/T_{AA}) - 2S_X^0}{(T_{AX}/T_- - T_{AX}/T_+)}$$

$$P' = P(T_{AX}/T_+ - T_{AX}/T_{AA})$$

$$Q' = Q(T_{AX}/T_- - T_{AX}/T_{AA})$$

In principle the recovery of S_A and S_X is non-exponential, but previous studies[12] of relaxation in AX_2 systems in small molecules have shown that when $R_{AX}/R_{XX} > 1.3$, as is the case here, the recovery is well described over the normally accessible region by a single exponential with effective relaxation times which we denote by T_{1A}^{eff} and T_{1X}^{eff}. This was confirmed by the computer calculations and experimental investigation described below. The procedure in the computer calculations was to calculate the recovery curve of S_A and S_X for a particular motional model, and then perform a least squares fit to a single exponential of the recovery curve extending from zero time to the time when the deviation from equilibrium had decreased to one quarter of its initial value.

I.r. experiment with decoupling. In this case, the cross-term in whichever of equations (3a) or (3b) applies to the unsaturated nucleus is held constant by the perturbing field. The relaxation of the unperturbed nucleus will therefore be exponential with a time constant T_{AA} in the case of A–{X} experiments or T_{XX} in the case of X–{A} experiments.

Nuclear overhauser effects. The steady state fractional enhancement of the methine proton when the methylene protons are saturated, η_A, is obtained by setting $\mathrm{d}S_A/\mathrm{d}t$ and S_X to zero in equation (4a), giving:

$$\eta_A = 2T_{AA}/T_{AX}$$

where we have used the relation $S_X^0 = 2S_A^0$. Similarly:

$$\eta_X = T_{XX}/2T_{XA}$$

Motional models

For the simple case of isotropic rotational diffusion,

$G(\tau)$ is exponential, with correlation time τ_c, and $J(\omega)$ is given by:

$$J(\omega) = \frac{\tau_c}{1 + \omega^2\tau_c^2}$$

In many cases however, polymer motion is better described by a distribution of correlation times[1,3]. Two such distributions have been employed previously. The Cole–Cole distribution[3,13,14], developed initially[13] for dielectric relaxation yields the following expression[14] for $J(\omega)$:

$$J(\omega) = \frac{1}{2\omega}\left[\frac{\cos(1-\gamma)\pi/2}{\cosh(\gamma \ln \omega\tau_0) + \sin(1-\gamma)\pi/2}\right]$$

τ_0 is the average correlation time and γ is the width parameter, $0 < \gamma < 1$. The case $\gamma = 1$ corresponds to the single correlation time model.

The log – χ^2 distribution, first applied by Schaefer[1] to ^{13}C relaxation gives the equation:

$$J(\omega) = \int_0^\infty \frac{\tau_0(pS)^{p-1}\exp(-pS)\,[\exp_b S - 1]\,\mathrm{d}S}{\Gamma(p)(b-1)\{1 + \omega^2\tau_0^2[(\exp_b S - 1)/(b-1)]^2\}}$$

where

$$S = \log_b[1 + (b-1)\tau_c/\tau_0]$$

τ_0 is again the average correlation time, and p the width parameter. The smaller p is, the wider the distribution, but for $p \geqslant 100$, this distribution is indistinguishable from the single correlation time model. The log base b is to some extent arbitrary[1], and we have chosen the value 1000 as used previously[3]. The integral is evaluated numerically.

The above distributions are simply a formal way of representing a non-exponential autocorrelation function, but one may also assume an analytic form for the autocorrelation function itself. One such form arises from a model[6] of polymer motion consisting of a combination of conformational jumps with the backbone carbon atoms confined to a tetrahedral lattice, and overall molecular tumbling. If the jump correlation time is τ_D, and the overall tumbling correlation time τ_0, the correlation function is[6]:

$$G(\tau) = \exp(-\tau/\tau_0)\exp(\tau/\tau_D)\,[1 - \mathrm{erf}(\tau/\tau_D)^{1/2}] \qquad (5)$$

Such a correlation function also arises for relaxation by jump diffusion of small molecules in solids[15], and yields[15]:

$$J(\omega) = \frac{\tau_0\tau_D(\tau_0 - \tau_D)}{(\tau_0 - \tau_D)^2 + \omega^2\tau_0^2\tau_D^2} \left\{\left(\frac{\tau_0}{2\tau_D}\right)^{1/2} \times \left[\frac{(1+\omega^2\tau_0^2)^{1/2} + 1}{1 + \omega^2\tau_0^2}\right]^{1/2} + \left(\frac{\tau_0}{2\tau_D}\right)^{1/2} \times \frac{\omega\tau_0\tau_D}{(\tau_0 - \tau_D)}\left[\frac{(1+\omega^2\tau_0^2)^{1/2} - 1}{1 + \omega^2\tau_0^2}\right]^{1/2} - 1\right\}$$

Computer calculations

The relaxation times and Overhauser enhancements for each model have been calculated for different correlation times and distribution widths. To determine the distances as accurately as possible, calculations were made of the geometry of the most favoured conformations of sequences of six dyads of all possible tacticities. The conformational sequences were constructed from the (*gt*) and (*tg*) conformations of isotactic dyads, and the (*tt*) and (*gg*) conformations of syndiotactic dyads with the proviso that adjacent dyad junctions of the type (*–g*)(*g–*) are forbidden[16]. The bond lengths and angles used were[17]:

r(C–H) = 0.1073 nm ; r(C–C) = 0.1541 nm

(C–C–C) = 112° ; (C–C–H) = 112°

The small displacement of the torsional angle from perfect staggering[16] due to steric interaction of large vicinal groups was taken to be 10°. The effective internuclear distances resulting from averaging over conformation and tacticity were:

$R_{AA} = 0.2726$ nm ; $R_{AX} = 0.2415$ nm

$R_{XX} = 0.1660$ nm

The reliability of these distances is considered more fully in the Discussion below. Calculations of relaxation times and Overhauser enhancements were performed for ω_A = 300.25 MHz and $\omega_A - \omega_X$ = 930 Hz, this being the chemical shift observed in poly(vinyl acetate) used in the experimental part of this work. Relaxation times $T_{1A}^{\rm eff}$, $T_{1X}^{\rm eff}$, T_{AA} and T_{XX} are shown in *Figure 1* for the log – χ^2 distribution as a function of τ_0 and p. *Figure 2* shows the corresponding Overhauser effects, and *Figures 3* and *4* show analogous results for the conformational jump model as a function of τ_0 and τ_D. Results for the Cole–Cole distribution are not shown, for they are very similar to the log – χ^2

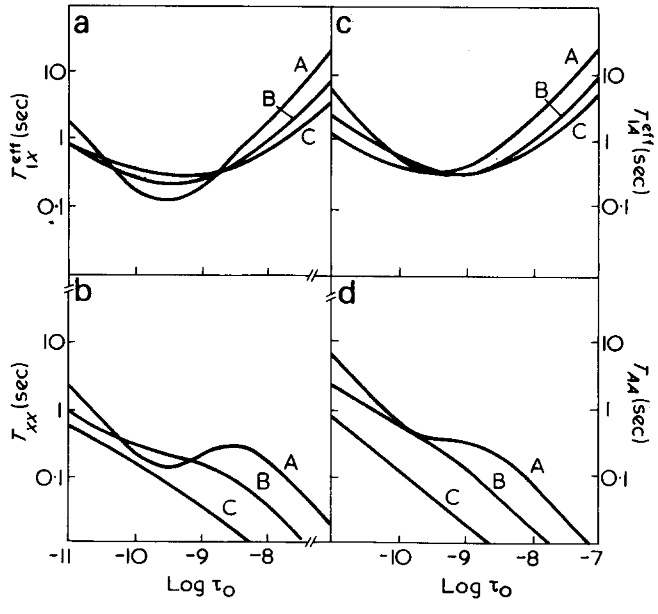

Figure 1 Plots of (a) $T_{1X}^{\rm eff}$; (b) T_{XX}; (c) $T_{1A}^{\rm eff}$ and (d) T_{AA} vs. τ_0 for the log – χ^2 distribution of correlation times. Values of p: A, ∞; B, 20; C, 10

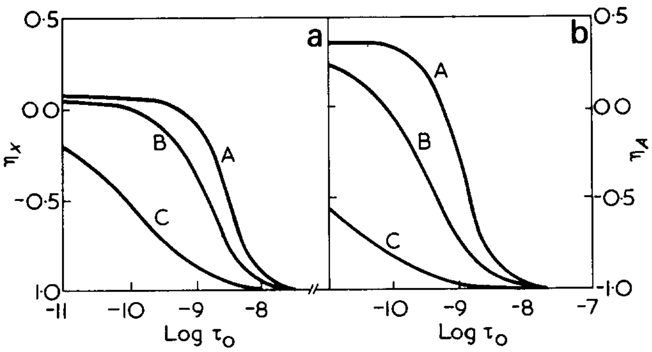

Figure 2 Plots of (a) η_X and (b) η_A vs. τ_0 for the log – χ^2 distribution of correlation times. Values of p: A, ∞; B, 20; C, 10

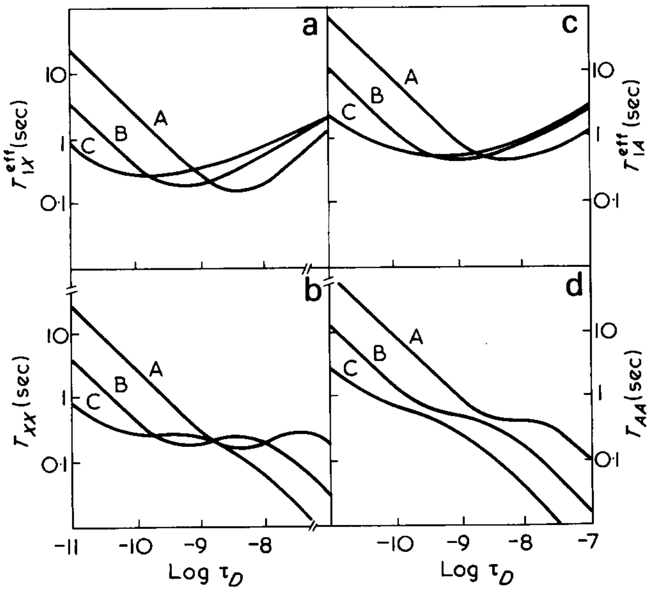

Figure 3 Plots of (a) $T_{1X}^{\rm eff}$; (b) T_{XX}; (c) $T_{1A}^{\rm eff}$ and (d) T_{AA} vs. τ_D for the conformational jump model. Values of τ_D/τ_0: A, 10.0; B, 1.0, C, 0.1

distribution. Before describing the effects of a correlation time distribution, it is worthwhile pointing out several notable features of the relaxation data for the single correlation time model, shown in *Figures 1* and *2* as the limit of the log – χ^2 distribution when $p \to \infty$. Firstly, $T_{1A}^{\rm eff}$ and $T_{1X}^{\rm eff}$ pass through a minimum, whereas T_{AA} is a monotonic function of τ_c and T_{XX} passes through a minimum and a maximum. T_{AA} and T_{XX} resemble spin–spin relaxation times. Secondly, $T_{1A}^{\rm eff}$ and $T_{1X}^{\rm eff}$ differ considerably on the short correlation time side of their minima but are equal on the long correlation time side. Thirdly, η_A and η_X fall sharply in the region of the minima in $T_{1A}^{\rm eff}$ and $T_{1X}^{\rm eff}$ from maximum values of 0.37 for η_A and 0.1 for η_X to minimum values of –1 in both cases. All these features are due to the variation in relative magnitude of $J(\omega_A - \omega_X)$ to the other $J(\omega)$ values. At short correlation times, such that $(\omega_A + \omega_X)^2\tau_c^2 \ll 1, J(\omega)$ is independent of ω. Because $r_{XX}/r_{AX} \sim 1.5$, the X–X dipolar contribution dominates the X relaxation, and the crossrelaxation term for X relaxation is negligible. Because the X relaxation is so much more efficient than the A relaxation, $(S_X - S_X{}^0)$ during the major part of the A recovery is very small, so the cross-relaxation term in the A relaxation is also of minor importance. Hence the effective relaxation times are very close to T_{AA} and T_{XX} which approximately differ by the factor $3r_{AX}^6/8r_{XX}^6 \sim 3.6$. η_A reaches a maximum value of 0.37 because the A relaxation is dominated by A–X dipolar interactions, whereas η_X is much smaller because A–X interactions are much less efficient than X–X in relaxing the X spins[11].

In the opposite case of long correlation times, when $(\omega_A + \omega_X)^2\tau_c^2 \gg 1, J(\omega_A - \omega_X)$ becomes very much larger than any other $J(\omega)$. In the unperturbed i.r. experiment, the equalization of spin temperature throughout the A–X spin system then proceeds much more rapidly than equilibration with the lattice, with the result that both A and X nuclei relax at the same rate, which is the spin–lattice relaxation rate of the most efficient sink i.e. the X nuclei. However, in the case of the decoupled i.r. experiment, the irradiated nucleus is very strongly coupled to the 'lattice' which now includes the decoupling field, and the relaxation rate of the unirradiated nucleus is the rate at which excess spin energy is transferred to the irradiated nucleus i.e. effectively the spin–spin relaxation time. The nuclear Overhauser enhancements become –1 because of transfer of saturation by efficient spin–spin relaxation.

Turning to the effects of a log – χ^2 distribution, the features noted above arising from the relatively large magnitude of $J(\omega_A - \omega_X)$ are even more marked, due to the increasing weighting of motions with longer correlation times. As the distribution becomes wider, the minimum in $T_{1X}^{\rm eff}$ is raised and broadened. The minimum in $T_{1A}^{\rm eff}$ is also broadened, but falls to lower values, reflecting the increase in efficiency of spin–lattice relaxation via spin–spin relaxation with the X spins. For the same reason, T_{AA} and T_{XX} also fall with increasing width, and likewise the nuclear Overhauser effects.

The conformational jump model is similar to the log – χ^2 distribution in some respects, but significantly different in others, as shown in *Figures 3* and *4*, where the relaxation parameters are plotted as a function of the jump correlation time τ_D for different values of the ratio τ_D/τ_0. When $\tau_D/\tau_0 > 100$, the model is effectively identical to the single correlation time model, and as τ_D/τ_0 decreases, the autocorrelation function departs further from an exponential. Reducing τ_D/τ_0 therefore is analogous to broadening a distribution of correlation times. As τ_D/τ_0 decreases, the minimum in $T_{1X}^{\rm eff}$ is raised and broadened, as for the log – χ^2 distribution, but the level of the minimum in $T_{1A}^{\rm eff}$ is practically unaffected. T_{AA} and T_{XX} decrease, and so do the Overhauser enhancements, though there is always a fairly sharp step in the latter, unlike the curves for the log – χ^2 distribution which show a very broad transition for the larger distribution widths.

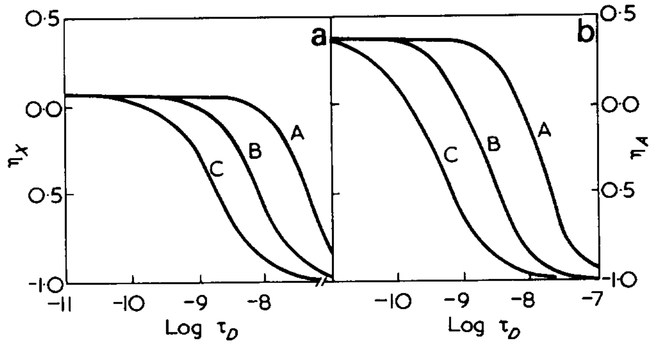

Figure 4 Plots of (a) η_X and (b) η_A vs. τ_D for the conformational jump model. Values of τ_D/τ_0: A, 10.0; B, 1.0; C. 0.1

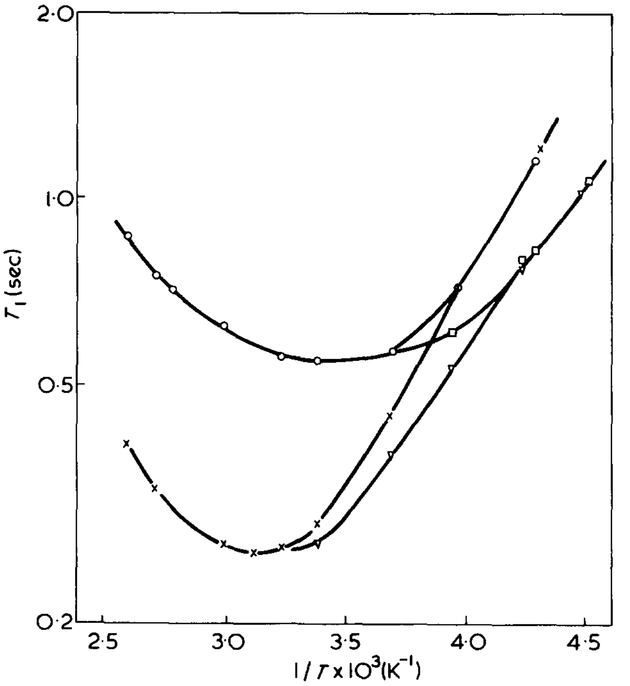

Figure 5 T_{1A}^{eff} and T_{1X}^{eff} vs. temperature for PVAC in toluene-d_8. ○, T_{1A}^{eff}, 134 mg/ml; X, T_{1X}^{eff}, 134 mg/ml; □, T_{1A}^{eff}, 17 mg/ml; ▽, T_{1X}^{eff}, 17 mg/ml. At the higher temperatures, the relaxation times are practically independent of concentration

It is clear from these calculations that measurements of the type described are sensitive to the nature of the correlation function, and that detailed information on its form may be obtained. We have made initial measurements on poly(vinyl acetate) in toluene-d_8 solution as a function of temperature and concentration. Poly(vinyl acetate) (PVAC) was chosen because the CH and CH_2 groups are well resolved[18], stereochemical shifts are fairly small[18], and the protons in the side group are far removed from those in the backbone.

EXPERIMENTAL

PVAC of $M_w = 45\,000$ was supplied by Koch-Light Laboratories Colnbrook, UK. The ^1H n.m.r. spectra indicated random tacticity[18], with a syndiotactic to isotactic dyad ratio of approximately 2:1. ^1H and ^{13}C relaxation measurements were made on Varian Associates SC-300 and XL-100 spectrometers respectively. Relaxation times were obtained using the standard π—τ—$\pi/2$ sequence, and ^1H Overhauser enhancements were obtained from the ratio of intensities of spectra recorded first with the appropriate group saturated and then with the decoupling frequency shifted an equal distance to the other side of the monitored group. Experimental errors were less than 10%.

RESULTS AND DISCUSSION

Experimental results for two solutions of PVAC in toluene-d_8 are shown in *Figures 5–7*.

At temperatures above 10°C, the data is practically independent of concentration, in agreement with previous studies[7,19], of polymer motion in solution, but at lower temperatures the results for the two solutions differ significantly indicating a concentration dependence of the polymer motion.

The curves are of the same form as those calculated for correlation times of the order of 10^{-8} to 10^{-10} sec. Thus T_{1A}^{eff} and T_{1X}^{eff} both exhibit broad minima, and become equal at the lower temperatures. The minimum for T_{1A}^{eff} occurs at a low temperature (i.e. longer correlation times) than that for T_{1X}^{eff}, as predicted. T_{AA} and T_{XX}, approximately equal to T_{1A}^{eff} and T_{1X}^{eff} respectively, at higher temperatures, decrease as the temperature falls. T_{AA} passes through an inflection, while T_{XX} shows the minimum/maximum structure calculated for the narrower distribution models described above. The Overhauser effects are negative over most of the temperature range, with η_X generally larger than η_A, except at the highest temperatures. Again this behaviour is in accord with the calculations.

Several features of these curves are clear evidence for the existence of a distribution of correlation times. In particular, we would mention the minimum value of T_{1X}^{eff}, experimentally 260 msec compared with the value of 130 msec calculated for a single correlation time, and also the ratio between the maximum and minimum values of T_{XX}. Experimentally this ratio is $\leqslant 1.4$ compared with the calculated value of 2.1.

Having established the qualitative correspondence between calculated and experimental relaxation data, we turn our attention to the quantitative relationship. We consider first the quantitative reliability of the calculations. The main uncertainty lies in the internuclear distances. Of these, R_{XX}^g is the most reliable, and since the *geminal* interaction dominates the X relaxation, then the values of T_{1X}^{eff}

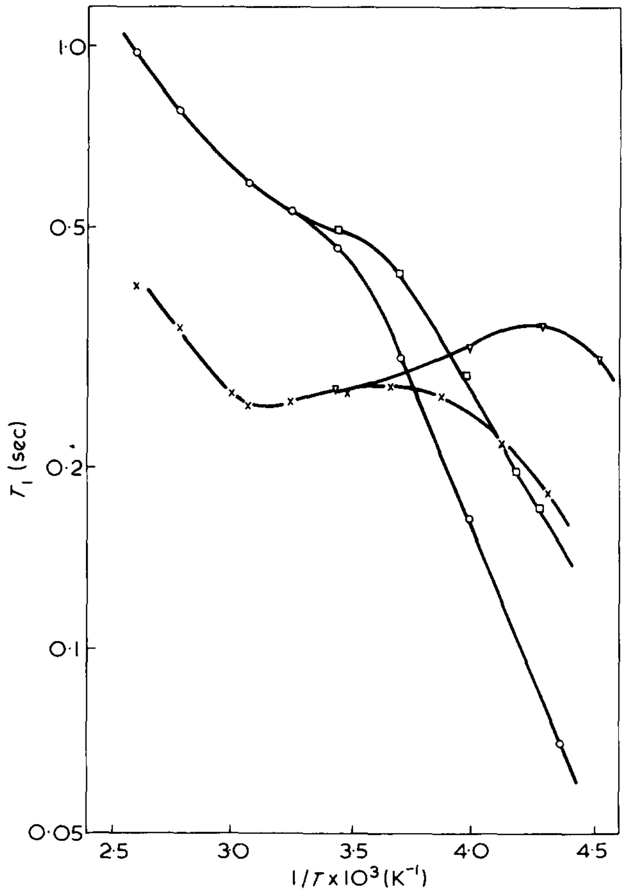

Figure 6 T_{AA} and T_{XX} vs. temperature for PVAC in toluene-d_8. ○, T_{AA}, 134 mg/ml; X, T_{XX}, 134 mg/ml; □, T_{AA}, 17 mg/ml; ▽, T_{XX}, 17 mg/ml. At the higher temperatures, the relaxation times are practically independent of concentration

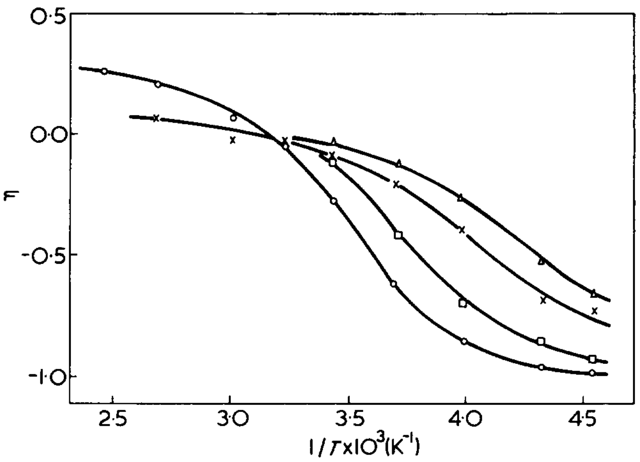

Figure 7 η_A and η_X vs. temperature for PVAC in toluene-d_8. ○, η_A, 134 mg/ml; X, η_X, 134 mg/ml; □, η_A, 17 mg/ml; △, η_X, 17 mg/ml

Table 1 Attempted fit of experimental data at 30°C (minimum in T_{1X}^{eff}). Relaxation times in msec. Solution concentration 17 mg/ml

Datum	Experi-mental	Cole–Cole[a]	Log – χ^2[b]	Conforma-tional jump[c]
T_{1A}^{eff}	540	305	370	610
T_{1X}^{eff}	260	(260)	(260)	(260)
T_{AA}	550	90	230	620
T_{XX}	250	85	150	260
η_A	0	–0.8	–0.55	0.01
η_X	0	–0.6	–0.3	0.03

[a] $\gamma = 0.7$; $\tau_0 = 3.3 \times 10^{-10}$ sec. [b] $p = 17$; $\tau_0 = 4 \times 10^{-10}$ sec.
[c] $\tau_D/\tau_0 = 0.1$; $\tau_D = 1.5 \times 10^{-10}$ sec

are reasonably accurate, to within 10%. The remaining parameters depend to a greater or lesser extent on the other distances, particularly R_{AX}. Uncertainties here arise from imprecise bond and torsion angles, and from the lack of information on the exact configurational and conformational structure of PVAC. A study of model compounds[20] of this polymer has shown that the major conformations of isotactic and syndiotactic units are those described earlier but the (*tt*) and (*gg*) forms are not equally weighted. However, a series of calculations with a reasonable range of structural parameters showed that the values of R_{AX} and R_{AA} are sufficiently accurate to establish the relaxation times T_{1A}^{eff}, T_{AA} and T_{XX} to within 30%. It was found that the ratio R_{AX}/R_{AA} remained fairly constant, so that η_A can be calculated more accurately.

Our general procedure in attempting to fit the experimental data at a given temperature to a particular model was first to determine the correlation time for that model which reproduced the observed value of T_{1X}^{eff}, and then to compare the values of the remaining relaxation parameters predicted using that correlation time and width with their experimental values. At certain temperatures, the shape of the curve determines the characteristics of the model. For example, at the temperature of the minimum in T_{1X}^{eff}, the value of T_{1X}^{eff} immediately fixes the width of the distribution, since the depth of this minimum is strongly dependent on the width. At intermediate temperatures in the vicinity of the minima in T_{1A}^{eff} and T_{1X}^{eff}, it was found impossible to fit all the data to any Cole–Cole or log – χ^2 distribution. Only the conformational jump model provided a satisfactory interpretation, as shown for the more dilute solution in *Tables 1* and *2*. In *Table 1*, the distribution parameters used are those reproducing the observed minimum value of T_{1X}^{eff}. For the Cole–Cole and log – χ^2 distributions, T_{1X}^{eff} is reproduced only by parameters generating unacceptably low values of T_{AA}, T_{XX}, η_A and η_X. Distribution widths required to produce reasonable values of these four measurements give values for T_{1X}^{eff} of less than 180 msec, which is outside the range of experimental error.

In *Table 2*, the correlation times were fixed by the condition that T_{1A}^{eff} be a minimum, but the width parameters were chosen to give agreement between experimental and calculated values of T_{1X}^{eff}. Again only the jump model gives an acceptable fit to all the other parameters.

In *Table 3* we consider the interpretation of the data for the extremes of temperature. At the lowest temperatures, the data for the more dilute solution is matched very well by the single correlation time model (Column I). This model is also acceptable at the highest temperature (Column II) but is slightly inferior to the jump model with a τ_D/τ_0 ratio of about 0.07 (Column III). It is likely that at even higher temperatures the single correlation time model would be entirely satisfactory.

The behaviour of the more concentrated solution at high and intermediate temperatures was essentially identical to the less concentrated solution, but at low temperatures, the single correlation time model was unsatisfactory. At –45°C, for example, reasonable agreement was obtained for the conformational jump model with $\tau_D/\tau_0 = 10$ and $\tau_D = 1.5 \times 10^{-7}$ sec, giving calculated values for T_{1A}^{eff}, T_{1X}^{eff}, T_{AA},

Table 2 Attempted fit of data at 10°C (minimum in T_{1A}^{eff}). Relaxation times in msec. Solution concentration 17 mg/ml

Datum	Experi-mental	Cole–Cole[a]	Log – χ^2[b]	Conforma-tional jump[c]
T_{1A}^{eff}	520	310	340	450
T_{1X}^{eff}	300	310	280	250
T_{AA}	470	16	150	400
T_{XX}	270	28	150	220
η_A	–0.25	–0.97	–0.73	–0.2
η_X	–0.08	–0.89	–0.37	–0.05

[a] $\gamma = 0.6$; $\tau_0 = 3.5 \times 10^{-10}$ sec. [b] $p = 20$; $\tau_0 = 9.2 \times 10^{-10}$ sec.
[c] $\tau_D/\tau_0 = 0.3$; $\tau_D = 7.5 \times 10^{-10}$ sec

Table 3 Fit of experimental data at high and low temperatures. Relaxation times in msec. Solution concentration 17 mg/ml

	I[a] –45°C		II[b] 110°C		III[c] 110°C	
Datum	Calc.	Exp.	Calc.	Exp.	Calc.	Exp.
T_{1A}^{eff}	930	930	1100	860	1050	860
T_{1X}^{eff}	(930)	930	(390)	390	(390)	390
T_{AA}	140	180	1300	970	1150	970
T_{XX}	290	330	430	400	420	400
η_A	–0.88	–0.9	0.36	0.23	0.25	0.23
η_X	–0.63	–0.6	0.06	0.07	0.05	0.07

[a] Column I: single correlation time, $\tau_c = 4 \times 10^{-9}$ sec. [b] Column II: single correlation time, $\tau_c = 5 \times 10^{-11}$ sec. [c] Column III: conformational jump model, $\tau_D/\tau_0 = 0.07$, $\tau_D = 3 \times 10^{-11}$ sec

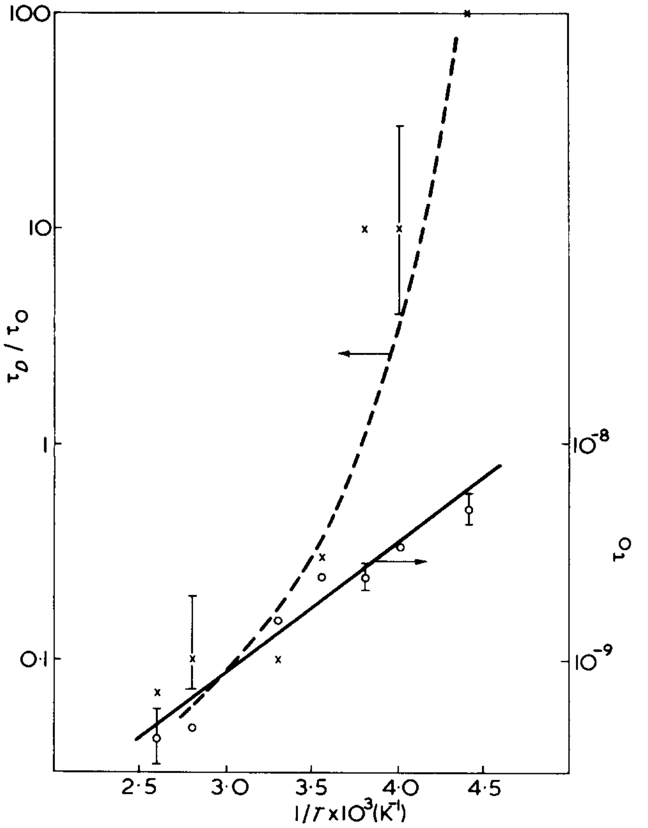

Figure 8 Plots of τ_0(O) and τ_D/τ_0(x) vs. $1/T$ for the 17 mg/ml solution of PVAC in toluene-d_8

T_{XX}, η_A and η_X of respectively 1400, 1400, 73, 130, –0.97 and –0.89, compared with experimental values of 1400, 1400, 65, 160, –0.95 and –0.72 (relaxation times in msec).

These results demonstrate that a variety of relaxation measurements can be interpreted successfully by the two parameter conformational jump model, which is clearly superior to others used in the analysis of polymer motion. The difference between models is revealed by the difference between the spectral densities at high and low frequencies, as reflected in the relative values of T_{1X}^{eff} and the group of parameters (T_{AA}, T_{XX}, η_A, η_X). The parameters for the conformational jump model in *Table 1* are also successful in predicting ^{13}C relaxation times and Overhauser enhancements[3]. For a ^{13}CH group at 25 MHz, the calculated T_{1C} is 170 msec and the nuclear Overhauser enhancement factor η_C is 1.6. The experimental values for the CH carbon in a dilute toluene-d_8 solution at 30°C are 150 ± 15 msec and 1.6 ± 0.2, respectively.

The results described here have shown that for this particular system the single correlation time model is adequate at temperatures well removed from the minima in T_{1A}^{eff} and T_{1X}^{eff}, but in the vicinity of these minima, the autocorrelation function is perceptibly non-exponential and is well described by the conformational jump model. A possible explanation of this behaviour is as follows. We note first that the conformational jump model reduces to the single correlation time model whenever either (a) $\omega\tau_0, \omega\tau_D \ll 1$ or (b) $\tau_0 \ll \tau_D$. In case (a), the function $J(\omega)$ reduces to:

$$J(\omega) = \frac{\tau_0(\tau_D)^{1/2}}{(\tau_0)^{1/2} + (\tau_D)^{1/2}}$$

i.e. independent of frequency. The ratio τ_D/τ_0 cannot therefore be determined, only a mean correlation time defined by the above expression. In case (b), the exponential decay dominates the autocorrelation function and $J(\omega)$ becomes:

$$J(\omega) = \frac{\tau_0}{1 + \omega^2\tau_0^2}$$

i.e. the single correlation time form. Now at temperatures near the T_{1A}^{eff} and T_{1X}^{eff} minima, where both the ratio τ_D/τ_0 and τ_D can be determined τ_D/τ_0 increases as the temperature decreases. We therefore ascribe the validity of a single correlation time at higher temperatures to the fact that $\omega\tau_0, \omega\tau_D \ll 1$, and at lower temperatures to the fact that $\tau_0 \ll \tau_D$. This implies that the activation energy for $\tau_D(E_D)$ is much greater than for $\tau_0(E_0)$ i.e. the barrier to conformational jumps is larger than the activation energy for the large scale tumbling motions. The latter are probably determined by the solvent viscosity and one may therefore expect that E_0 is comparable in magnitude to the activation energy for viscosity. *Figure 8* shows Arrhenius plots of τ_0 and τ_D/τ_0 for the less concentrated solution with some typical errors indicated. The straight line for log τ_0 vs. $1/T$ yields an activation energy of 11 ± 2 kJ/mol which is comparable to the value of 9 kJ/mol for the viscosity of toluene[21]. The ratio τ_D/τ_0 appears to undergo a very rapid increase as the temperature falls, which may be due to a freezing out of conformational jumps, as in the glass transition. It is noteworthy that at the lower temperatures the relaxation times become concentration dependent, and the value of τ_D/τ_0 decreases with increasing concentration. This is consistent with the view that at lower temperatures, large scale viscosity dependent motions dominate the relaxation mechanism.

ACKNOWLEDGEMENTS

The authors would like to express their gratitude to the Science Research Council for a Studentship to M. K. C. and for funding the n.m.r. spectrometers, and to Professor G. Allen and R. F. Warren for helpful advice and discussion.

REFERENCES

1 Schaefer, J. *Macromolecules* 1973, **6**, 882
2 Hermann, G. and Weill, G. *Macromolecules* 1975, **8**, 171
3 Heatley, F. and Begum, A. *Polymer* 1976, **17**, 399
4 Cutnell, J. D. and Glasel, J. A. *Macromolecules* 1976, **9**, 71
5 Preissing, G. and Noack, F. *Progr, Colloid Polym. Sci.* 1975, **57**, 216
6 Valeur, B., Jarry, J.-P., Geny, F. and Monnerie, L. *J. Polym. Sci. (Polym. Phys. Edn)* 1975, **13**, 667, 675, 2251
7 Anderson, J. E., Liu, K.-J. and Ullman, R. *Discuss. Faraday Soc.* 1970, **49**, 257
8 Heatley, F. and Walton, I. *Polymer* 1976, **17**, 1019
9 Doddrell, D., Glushko, V. and Allerhand, A. *J. Chem. Phys.* 1972, **56**, 3683
10 Vold, R. L., Vold, R. R. and Simon, H. E. *J. Magn. Reson.* 1973, **11**, 283
11 Noggle, J. H. and Schirmer, R. E. 'The Nuclear Overhauser Effect', Academic Press, New York, 1971
12 Scrivens, J. H. and Heatley, F. *JCS Faraday Trans. 2* in press
13 Cole, K. S. and Cole, R. H. *J. Chem. Phys.* 1941, **9**, 341

14 Connor, T. M. *Trans. Faraday Soc.* 1964, **60**, 1574

15 Hunt, B. I. and Powles, J. G. *Proc. Phys. Soc.* 1966, **88**, 513

16 Flory, P. J. 'Statistical Mechanics of Chain Molecules', Wiley–Interscience, New York, 1969

17 Sutton, L. E. 'Tables of Interactomic Distances', Special Publications 11 and 18, The Chemical Society, London, 1958 and 1965

18 Ramey, K. C. and Lini, D. C. *J. Polym. Sci. (Polym. Lett Edn)*, 1967, **5**, 39

19 Heatley, F. *Polymer* 1975, **16**, 493

20 Doskocilova, D., Stokr, J., Votavova, E., Schneider, B. and Lim, D. *J. Polym. Sci. (C)* 1967, **16**, 2225

21 'Handbook of Chemistry and Physics', 50th Edn, The Chemical Rubber Company, Cleveland, 1969